International Journal of Scientific Research in Mathematical and Statistical Sciences
Vol.**11**, Issue.**3**, pp.**57-63**, June **2024**
E-ISSN: 2348-4519
Available online at: www.isroset.org

Research Article

Fractional Mathematical Modeling of Ternary Nanofluid Flow Through an Inclined Artery

Hamza Saleh Zakari[1], Aminu Barde[2], Isah Abdullahi[3*]

[1,2,3]Dept. of Mathematical Sciences, Abubakar Tafawa Balewa University, Bauchi, Nigeria

**Corresponding Author: isahabdullahi7474@gmail.com, Tel: +2347039747474*

Received: 15/Apr/2024; **Accepted**: 17/May/2024; **Published**: 30/Jun/2024

Abstract— In this study, we examined the fractional order flow of Casson tri-nanofluid through an inclined artery, integrating gold (Au), copper (Cu), and alumina (Al_2O_3) nanoparticles into blood to form the tri-nanofluid. The flow was modelled as highly pulsatile. The mathematical formulation used differential forms of the conservation laws of mass, momentum, and energy, with the electric potential along the arterial wall accurately described by the Poisson-Boltzmann equation. The classical problem was converted into its fractional equivalents using the Caputo time-fractional derivative. Exact solutions for these transformed equations were derived using a combination of Laplace and finite Hankel transforms, with results computed and graphically presented using Mathcad software. The purpose of incorporating the tri-nanofluid was to enhance heat transfer by improving the fluid's thermal conductance. The findings revealed that the velocity profiles of the blood flow decreased with an increasing radiation parameter, while the opposite effect was observed with increasing porosity parameter. The temperature profile arose with higher fractional parameter values. This study holds potential for applications in targeted drug delivery using magnetic nanoparticles..

Keywords— Nano Particles, Inclined Artery, Ternary nanofluid, Time-Fractional Derivative

1. Introduction

Fluids with low molecular weights, like water, and air, are classified as Newtonian fluids, characterized by a linear stress-strain rate relationship described by the Navier-Stokes equation. However, many fluids, such as polymer solutions, multi-grade engine oils, toothpaste, liquid soaps blood, and peanut butter, do not adhere to this classification and are termed as non-Newtonian fluids due to their combination of viscous and elastic properties, exhibiting a nonlinear stress-strain rate relationship. The theoretical examination of non-Newtonian fluid flow remains significant in literature owing to their increasing relevance in modern technology and industries. Non-Newtonian fluid flows are prevalent in various applications, including industrial processes involving synthetic fibres, plastic extrusion, and polymer solution flows. Non-Newtonian fluids involved in heat transfer processes play crucial roles in polymer processing, thrust bearing and radial diffuser design, oil thermal recovery, transpiration cooling, drag reduction, drug delivery, to mention a few among others.

Due to the complex physical structure of non-Newtonian fluids, no single constitutive equation exists in the literature that can encompass all their flow properties. Consequently, numerous constitutive equations or models have been proposed, with significant attention given to Newtonian and non-Newtonian fluids. Pertinent contributions on these types of fluids have been made, by [1,2,3,4,5].

Blood, as non-Newtonian fluid, is crucial for life, mainly because it transports nutrients and oxygen throughout the body. It also plays a key role in removing metabolic waste products and carrying chemical signals to the kidneys for elimination. In the human circulatory system, the heart's rhythmic pumping creates a pulsatile pressure gradient that drives blood flow through the vessels. This pressure pulse, often measured at the wrist by physicians, reflects the heart's activity.

Importantly, blood also acts as a carrier of drugs to artery cell membranes, initiating chemical reactions between arterial cell and circulating fluids. Optimizing the compatibility of these biological reactions can significantly contribute to the development of therapeutic interventions. Despite the pivotal roles fulfilled by blood in the human circulatory system, there remains a substantial loss of human life attributed to various forms of cardiovascular diseases such as cancer, arigina, stroke e.t.c. [6]. It is evident that the study of blood flow in the presence of an applied magnetics and electric field has garnered significant attention from researchers because of its various applications in medical and physiological fields, as demonstrated by the works of [7,8,9,10]. Building on this established tradition, the current research seeks to explore a novel path by conducting an analysis of ternary nanofluid flow through an inclined artery using Caputo fractional derivative. The study aims to investigate the behavior of ternary hybrid nanofluids as they flow through an inclined artery under the influence of external magnetic fields and thermal radiation. This choice is motivated by the inherent characteristics of blood as a magnetic fluid, a concept previously acknowledged by [11,12,13,14,15,16]. Recognizing blood's magnetic properties, this research seeks to further our understanding of its behavior within the context of ternary nanofluid flow, taking into consideration of Casson fluid, thermal radiation, heat metabolism absorption and the permeability of the inclined artery.

2. Related Work

Biomagnetic fluid dynamics (BFD) is a burgeoning field within fluid mechanics dedicated to exploring the movement of bio-fluids (like blood) in the presence of magnetic fields. This area of research holds significant importance in medicine, particularly in applications such as drug delivery utilizing magnetic particles and in the treatment of conditions like excessive bleeding and malignant tumors [17,18]. In a recent study by [19], the non-Newtonian Casson fluid model was employed to analyze the one-way flow of blood through vessels with porous mediums. Because blood conducts electricity, researchers in [20,21] considered it to behave as a non-Newtonian fluid with characteristics of magnetohydrodynamics (MHD). Lately, [22] investigated both the flow of blood through vessels containing porous mediums and the motion of nanoparticles subjected to periodic vibration. The study incorporated aspects such as the non-Newtonian biviscosity fluid model, the Soret and Dufour effects, thermal radiation, and the linear variation of chemical reaction to depict thermo-solute transport using Caputo fractional order derivatives. Analytical solutions were derived utilizing methods including the Laplace transform, finite Hankel transform, and their respective inverses.

3. Methodology

We consider a model of axially symmetric, unsteady, incompressible blood flow developed for an inclined stenosed artery. In this model, three types of nanoparticles Cu, Au, and $Al_2O_3$are suspended in the blood (base fluid) to create a new composite, Cu, Au, Al_2O_3 Blood (tri-nanofluid), as depicted in figure 1.

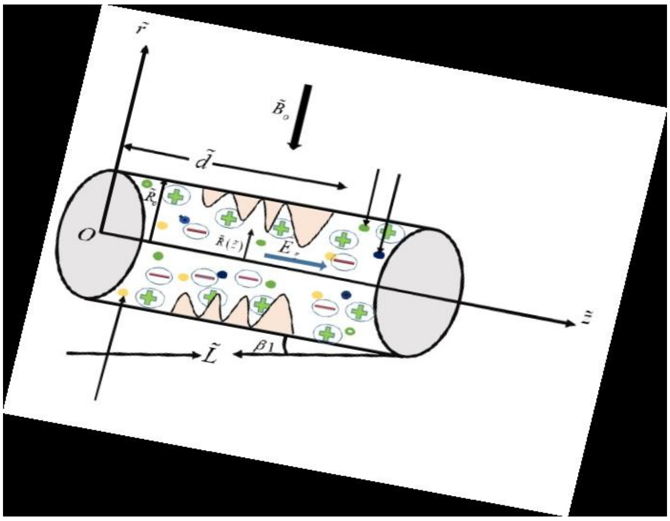

Fig. 1 Geometry of the physical problem

Newton's second law of motion demonstrates how Maxwell's equations and the movement of magnetic particles determine the strength of the magnetic field.

$$\left.\begin{aligned}&\rho_{thnf}\frac{\partial\bar{u}}{\partial\bar{t}}=-\frac{\partial\bar{p}}{\partial\bar{z}}+\mu_{thnf}\left(1+\frac{1}{\beta}\right)\left[\frac{\partial^2\bar{u}}{\partial\bar{r}^2}+\frac{1}{\bar{r}}\frac{\partial\bar{u}}{\partial\bar{r}}\right]+\rho_{thnf}G(\bar{t})-\\&\sigma_{thnf}B_0^2\bar{u}+\rho_eE_z+(\rho\sigma)_{thnf}g\sin\beta(\bar{T}-\bar{T}_\infty)-\frac{\mu_{thnf}}{k_p}\bar{u}\end{aligned}\right\}\quad(1)$$

$$\left.\begin{aligned}&(\rho C_p)_{thnf}\left[\frac{\partial\bar{T}}{\partial\bar{t}}+\bar{u}\frac{\partial\bar{T}}{\partial\bar{z}}+\bar{v}\frac{\partial\bar{T}}{\partial\bar{r}}\right]=K_{thnf}\left[\frac{\partial^2\bar{T}}{\partial\bar{r}^2}+\frac{1}{\bar{r}}\frac{\partial\bar{T}}{\partial\bar{r}}+\frac{\partial^2\bar{T}}{\partial\bar{z}^2}\right]\\&-\frac{\partial q_r}{\partial\bar{r}}+\bar{Q}_s+\theta_m\end{aligned}\right\}\quad(2)$$

The equation for the body acceleration in a vibrational environment is given by;

$$G(\bar{t})=\bar{A}_0\cos(\bar{k}\bar{t}+\Phi_0)\quad(3)$$

The model makes the following assumptions about the boundaries:

$$\left.\begin{aligned}&\bar{u}(\bar{r},\bar{t})=0 && when\quad \bar{r}=R(\bar{z})\\&\frac{\partial\bar{u}}{\partial\bar{r}}=0 && when\quad \bar{r}=0\\&\bar{T}(\bar{r},\bar{t})=T_w && when\quad \bar{r}=R(\bar{z})\\&\frac{\partial\bar{T}}{\partial\bar{r}}=0 && when\quad \bar{r}=0\end{aligned}\right\}\quad(4)$$

From Equation (1) and (2), we define the pressure gradient and heat radiation respectively as follows:

$$\frac{\partial\bar{p}}{\partial\bar{z}}=\bar{a}_0+\bar{a}_1\cos\left(\varpi\bar{t}\right)\quad(5)$$

$$-\frac{\partial q_r}{\partial\bar{r}}=4\alpha^2\left(\bar{T}-T_\infty\right)\quad(6)$$

When an electric field is applied axially to a nanofluid, an electrical double layer (EDL) forms at the vessel walls, generating a net electrical body force ($\rho_e E_z$). The Poisson equation describes the connection between electric potential $\tilde{\psi}$ and net charge density, ρ_e

$$\nabla^2 \bar{\varphi}(\bar{r}) = \frac{1}{\bar{r}} \frac{\partial}{\partial \bar{r}} \left(\bar{r} \frac{\partial \bar{\varphi}(\bar{r})}{\partial \bar{r}} \right) = -\frac{\bar{\rho}_e}{\varepsilon} \tag{7}$$

Where ε represents dielectric constant.
Equation (7) is known as the Boltzmann equation with the boundary conditions and the net charge density given as;

$$\left.\bar{\varphi}(1) = \varphi_\omega, \quad and \quad \frac{\partial \bar{\varphi}}{\partial \bar{r}} = 0, at \quad r = 0 \right\} \tag{8}$$

$$\bar{\rho}_e(\bar{r}) = e_0 \left(n^+ - n^- \right) = \frac{-2 z_0^2 e_0 n_0 \bar{\varphi}(\bar{r})}{k_g T_C} \tag{9}$$

Here ρ_e is the dielectric constant, $z_0, n_0, e_{0,} k_g$, n^+ and n^- are the ion valence, concentration of ions, the electronic charge, the Boltzmann constant the local absolute temperature of the fluid, the density number of cations and anions, respectively.
Using Debye–H$\ddot{u}$ckelparameter

$$\bar{k}^2 = \frac{2 z_0^2 c_0^2 n_0 \bar{\varphi}(\bar{r})}{c k_g T_0}$$

And the linearized Boltzmann equation (7), we get the electric field potential equation as:

$$\frac{1}{\bar{r}} \frac{\partial}{\partial \bar{r}} \left(\bar{r} \frac{\partial \bar{\varphi}(\bar{r})}{\partial \bar{r}} \right) = \bar{k}^2 \bar{\varphi}(\bar{r}) \tag{10}$$

The solution of equation (10) subject to the boundary conditions in (8) is given by:

$$\varphi(r) = \frac{I_0(Ker)}{I_0(KeR)} \tag{11}$$

The The Caputo-Fabrizio derivative with fractional order $\alpha \epsilon (0,1)$ is define as:

$$^{CF}D_t^\alpha f(t) = \frac{M(\alpha)}{1-\alpha} \int_0^1 \exp\left[\frac{-\alpha(t-\tau)}{1-\alpha} \right] f(\tau) d\tau \tag{12}$$

The dimensionless parameters that are under consideration in the context of dimensionless initial and boundary conditions are:

$$\left.\begin{array}{l} r = \dfrac{\bar{r}}{R_0}, z = \dfrac{\bar{z}}{R_0}, \omega = \dfrac{\omega_2}{\omega_1} t = \dfrac{u_0 \bar{t}}{R_0}, u = \dfrac{\bar{u}}{u_0}, p = \dfrac{\bar{p}}{\rho u_0^2} \\ \theta = \dfrac{\bar{T} - T_\infty}{T_w - T_\infty}, A_0 = \dfrac{R_0 \bar{A}_0}{u_0^2}, k = \dfrac{\bar{k} R_0}{u_0}, u_e = \dfrac{\bar{E}_{\bar{z}} \bar{\varepsilon} \bar{\varphi}_w}{\mu_f} \\ Q_0 = \dfrac{R_0 \bar{Q}_0}{u_0 \rho \bar{C} p (T_w - T_\infty)}, \theta_0 = \dfrac{R_0 \bar{\theta}_0}{u_0 \rho \bar{C} p (T_w - T_\infty)} \end{array} \right\} \tag{13}$$

Utilizing the non-dimensional variable of Eq. (13) in Eqs. (1)-(2) after dropping the bars, assume
the following forms:

$$\left.\begin{array}{l} B_3 \lambda \dfrac{\partial u}{\partial t} = -\dfrac{\partial p}{\partial z} + B_4 \left(1 + \dfrac{1}{\beta} \right) \left[\dfrac{\partial^2 u}{\partial \bar{r}^2} + \dfrac{1}{r} \dfrac{\partial u}{\partial r} \right] + \\ B B_3 A_0 \cos(kt + \phi) - B_6 M^2 u + K e^2 \varphi(r) + \\ B_5 Gr \sin \beta\theta - \dfrac{B_4}{K} u \end{array} \right\} \tag{14}$$

$$B_1 Pe \left[\frac{\partial \theta}{\partial t} \right] = B_2 \left[\frac{\partial^2 \theta}{\partial r^2} + \frac{1}{r} \frac{\partial \theta}{\partial r} \right] + R\theta + Pe(Q_0 + \theta_0) \tag{15}$$

Where:

$$M^2 = \frac{\sigma_f B_0^2 R_0}{\mu_f}, \lambda = \frac{\rho_f \omega_1 R_0^2}{\mu_f}, \Pr = \frac{\mu_f C_p}{k_f},$$

$$Gr = \frac{\rho_f (\alpha_T)_f g (T - T_\infty) R_0^2}{\mu_f u_0}, \mathrm{Re} = \frac{R_0 u_0}{v},$$

$$K = \frac{k_p}{R_0^2}, R = \frac{4 \alpha_1^2 R_0^2}{k}, Pe = \mathrm{Re}.\Pr$$

Are defined as Hartman Number, Pulsatile Reynolds number, Prandtl number, Grashof number, Reynolds number, Darcy number, thermal radiation parameter and Peclet number respectively.
The boundary conditions in the non-dimensional form are:

$$\left.\begin{array}{lll} u(r,t) = 0 & when & r = R(z) \\ \dfrac{\partial u}{\partial r} = 0 & when & r = 0 \\ T(r,t) = T_w & when & r = R(z) \\ \dfrac{\partial T}{\partial r} = 0 & when & r = 0 \end{array} \right\} \tag{16}$$

The governing momentum and temperature equations are described in the time fractional model (12) as;

$$\left.\begin{array}{l} B_3 \lambda D_t^\alpha = a_0 + a_1 \cos(\omega t) + \\ B_4 \left(1 + \dfrac{1}{\beta} \right) \left[\dfrac{\partial^2 u}{\partial \bar{r}^2} + \dfrac{1}{r} \dfrac{\partial u}{\partial r} \right] + \\ B_3 A_0 \cos(kt + \phi) - B_6 M^2 u + \\ K e^2 \varphi(r) + \\ B_5 Gr \sin \beta\theta - \dfrac{B_4}{K} u \end{array} \right\} \tag{17}$$

$$B_1 Pe D_t^\alpha = B_2 \left[\frac{\partial^2 \theta}{\partial r^2} + \frac{1}{r} \frac{\partial \theta}{\partial r} \right] + R\theta + Pe(Q_0 + \theta_0) \tag{18}$$

Applying the combined Laplace transform and the zero-order Hankel Transform together with the conditions in (16), we obtain the following for equation (17)-(18):

$$\theta_H(r_n,s)=\frac{B_2(Q_0+\theta_m)}{sB_1}\left[\frac{1}{s^{\alpha}+A_{1n}}\right]\frac{J_1(r_n)}{r_n} \qquad (19)$$

$$u_H(r_n,s)=\left\{\begin{array}{l}\left[\begin{array}{l}\frac{a_0}{s}+\frac{a_1 s}{s^2+\omega^2}+\\ B_3A_0\left(\frac{s\cos\phi-k\sin\phi}{k^2+s^2}\right)\end{array}\right]\\ \frac{1}{B_3\lambda(s^{\alpha}+A_{2n})}\frac{J_1(r_n)}{r_n}+\\ \left[\frac{B_5Gr(Q_0+\theta_m)\sin\beta_1}{B_3\lambda(s^{\alpha}+A_{1n})(s^{\alpha}+A_{2n})}\right]\\ \frac{J_1(r_n)}{r_n}+\frac{r_nKe^2}{s(r_n^2+k^2)B_3\lambda}J_1(r_n)\end{array}\right\} \qquad (20)$$

Now by applying the invers Henkel transform to equations (19)- (20), we have:

$$\theta(r,s)=\frac{B_2(Q_0+\theta_m)}{sB_1}\left[\frac{1}{s^{\alpha}+A_{1n}}\right]\Delta(r) \qquad (21)$$

$$u(r,s)=\left\{\begin{array}{l}\left[\begin{array}{l}\frac{a_0}{s}+\frac{a_1 s}{s^2+\omega^2}+\\ B_3A_0\left(\frac{s\cos\phi-k\sin\phi}{k^2+s^2}\right)\end{array}\right]\\ \frac{1}{B_3\lambda(s^{\alpha}+A_{2n})}\Delta(r)+\\ \left[\frac{B_5Gr(Q_0+\theta_m)\sin\beta_1}{B_3\lambda(s^{\alpha}+A_{1n})(s^{\alpha}+A_{2n})}\right]\\ \Delta(r)+\frac{1}{sB_3\lambda}\Omega(r)\end{array}\right\} \qquad (22)$$

where

$$\Delta(r)=2\sum_{n=1}^{\infty}\frac{J_0(r_n,r)}{r_nJ_1(r_n)}$$

$$\Lambda(r)=2\sum_{n=1}^{\infty}\frac{kr_n}{r^2{}_n+k^2}\frac{J_0(r_n,r)}{r_nJ_1(r_n)}$$

The inverse Laplace form of equations (21) -(22) was taken with the aid of Gerby-Stefan's Algorithm and the results were simulated graphically with the aid of MATCARD software as shown in the next section.

5. Results and Discussion

In this section, we present and analyze the numerical results and graphical simulations depicting the behavior of ternary nanofluid flow through an inclined artery under the influence of electric and magnetic fields.

4o

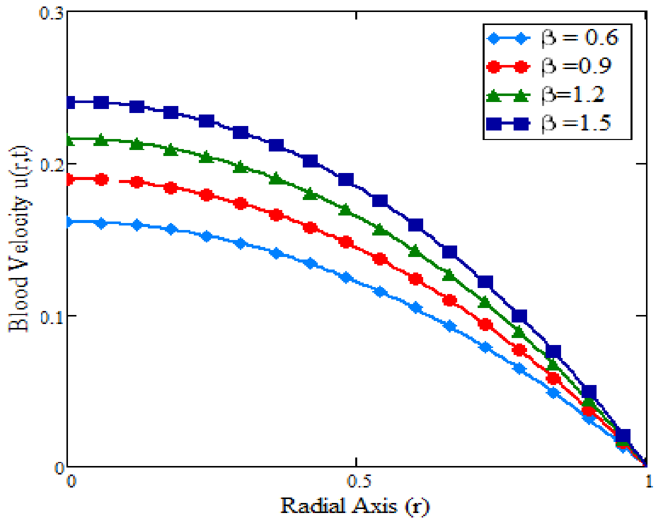

Figure 2: Blood velocity for various values of Casson fluid parameter

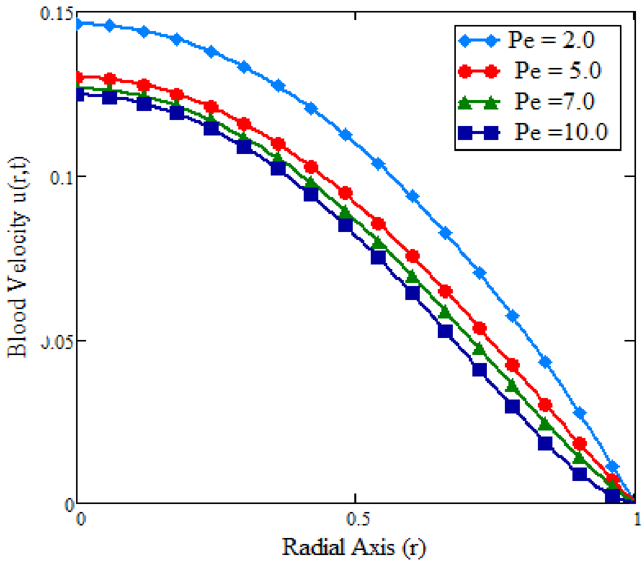

Figure 3: Blood velocity for various values of Peclet number

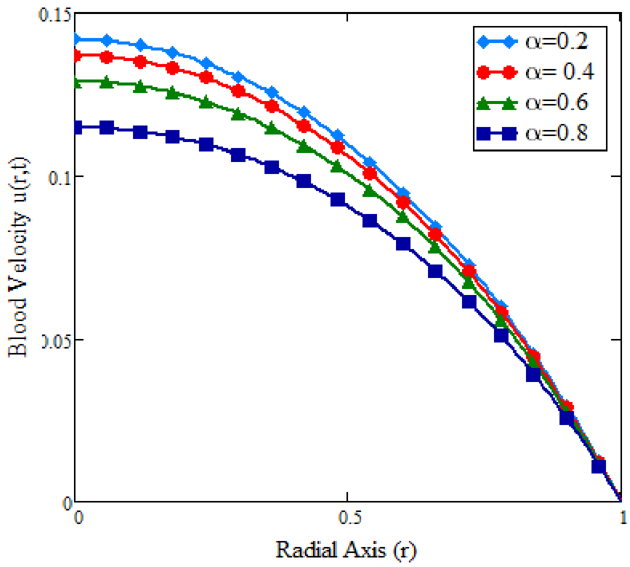

Figure 4: Blood velocity for various values of Fractional parameter

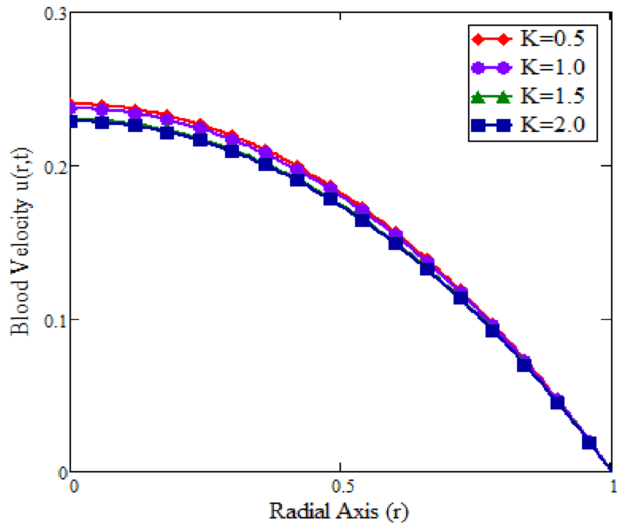

Figure 5: Blood velocity for various values of Porosity parameter

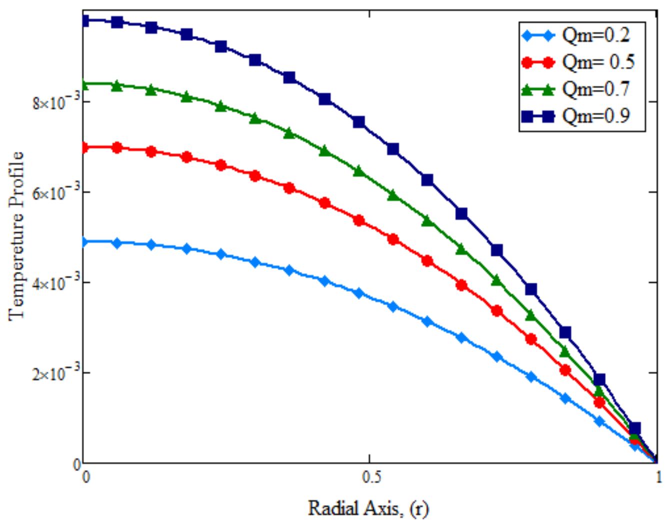

Figure 8: Temperature profile for various values of heat metabolism absorption parameter

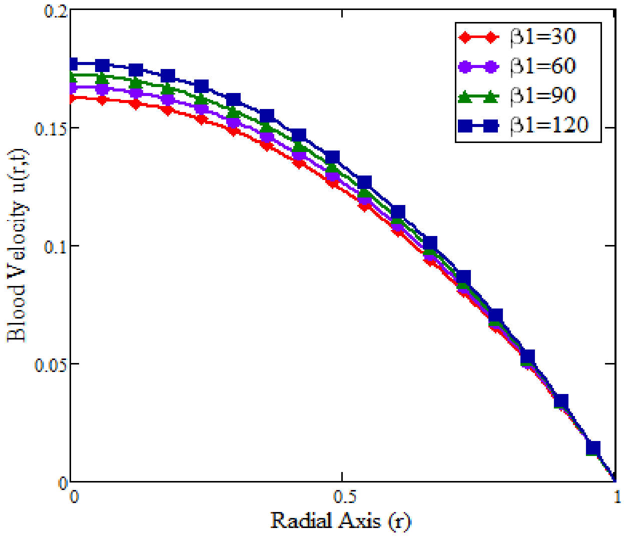

Figure 6: Blood velocity for various values angle of inclined artery

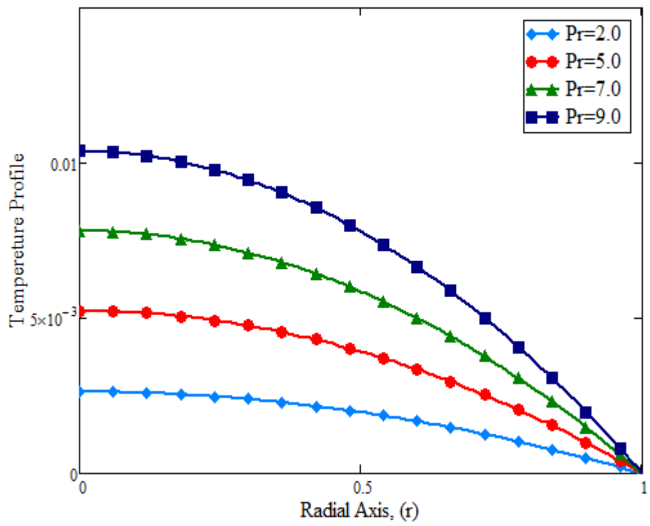

Figure 9: Temperature profile for various values Prandtl number

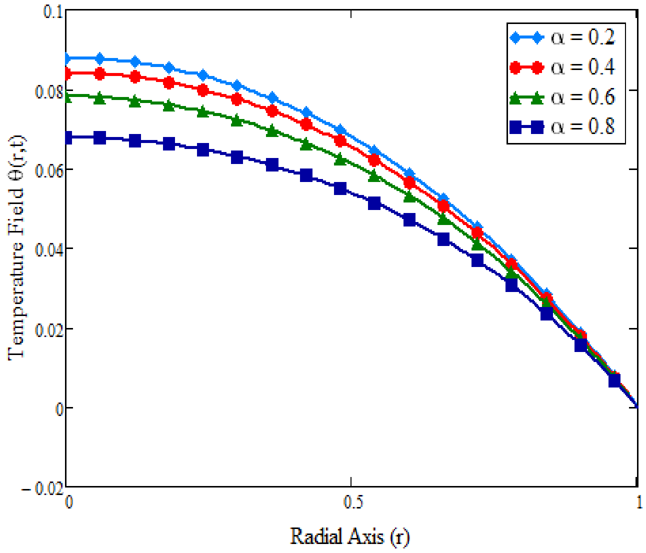

Figure 7: Temperature profile values Fractional parameter

Figure 2 explored how changes in the Casson fluid parameter impacted the blood velocity within the inclined artery. The Casson model, commonly used to describe the non-Newtonian behavior of fluids with yield stress, influenced the flow properties of such fluids. The plot in Figure 2 illustrated how the blood velocity varied across the inclined artery for different Casson fluid parameter values. Variations in the Casson fluid parameter affected the yield stress behavior of the ternary nanofluid, resulting in changes in flow patterns and velocity profiles.Figure 3 investigated how changes in the Peclet number influenced the blood velocity within the inclined artery. The Peclet number related the relative importance of convective transport to diffusive transport in the fluid flow, reflecting the balance between advection and diffusion processes. The plot in Figure 3 showed how the blood velocity varied across the inclined artery for different Peclet number values. Variations in the Peclet number impacted the dominance of convective or diffusive transport mechanisms, affecting the overall flow behavior and velocity profiles.Figure 4 explored how changes in the fractional parameter impacted the blood velocity within the inclined artery. The fractional parameter was associated with fractional calculus, introducing memory and non-local effects into the mathematical modeling of fluid dynamics. The plot in Figure 4 illustrated how the blood velocity varied across the inclined artery for different fractional parameter values. Variations in the fractional parameter led to changes in the velocity profiles, reflecting the non-integer order dynamics of the ternary nanofluid flow. Figure 5 investigated how changes in the porosity parameter affected the blood velocity within the inclined artery. The porosity parameter represented the fraction of void space in the porous medium, influencing the flow behavior and resistance to fluid motion. The plot in Figure 5 illustrated how the blood velocity varied across the inclined artery for different porosity parameter values. Alterations in porosity resulted in variations in flow velocities, indicating how the presence of void spaces impacted the fluid flow dynamics.The plot in Figure 6 showed how the blood velocity varied across the inclined artery for different angles of inclination. Higher or lower inclination angles could lead to variations in flow velocity profiles, affecting the fluid dynamics and transport properties within the artery. The temperature profile depicted in Figure 7 demonstrated how changes in the fractional parameter influenced the distribution of temperature along the flow domain of the inclined artery. Different fractional parameter values could lead to distinct temperature profiles, reflecting the complex nature of the fluid flow behavior. Figure 8 explored how different values of this parameter influenced the temperature distribution within the ternary nanofluid as it flowed through the inclined artery. The temperature profile showcased how the temperature varied across the flow domain of the inclined artery for varying heat metabolism absorption parameters. Changes in this parameter could lead to alterations in the heat absorption or release rates, affecting the overall thermal behavior of the fluid. In Figure 9, different values of the Prandtl number were considered, indicating variations in the relative rates of momentum and heat transfer within the ternary nanofluid. The temperature profile depicted in Figure 9 showcased how the temperature varied across the flow domain of the inclined artery for different Prandtl numbers. Higher Prandtl numbers typically indicated a higher thermal diffusivity relative to momentum diffusivity, leading to different temperature distributions within the fluid.

6. Conclusion and Future Scope

The analysis of blood flow in the context of ternary nanofluid dynamics within an inclined artery presents valuable insights into the complex interplay of fluid properties, rheological behavior, and transport phenomena. The findings across all figures provide a detailed examination of how variations in the Casson fluid parameter, Peclet number, and fractional parameter influence blood velocity and temperature profile within the artery, shedding light on the intricate dynamics of non-Newtonian fluid flow in biomedical applications. The findings underscore the significance of considering factors such as yield stress effects, convective-diffusive transport mechanisms, and fractional calculus in Modeling and understanding the behavior of ternary nanofluids in complex geometries. The research contributes to advancing knowledge in fluid dynamics, particularly in the context of biomedical applications were precise control over blood flow dynamics is crucial for therapeutic interventions.

Therefore**,** further exploration into the influence of magnetic and electric fields on ternary nanofluid flow dynamics in inclined arteries can expand the scope of research in bio magnetic fluid dynamics. Investigating the impact of external fields on blood velocity and transport properties can lead to advancements in targeted drug delivery and medical treatments. By addressing these recommendations and delving deeper into the complexities of ternary nanofluid flow in biomedical settings, researchers can further advance the understanding of fluid dynamics in physiological systems and pave the way for innovative applications in medical technology and treatment methodologies.

Availability of Data and Materials:
Not applicable

Conflict of Interest:
The authors declare that there are no conflicts of interest related to the study. This is an important declaration to ensure transparency and to address any potential biases that could arise from financial or personal relationships.

Funding:
The study received no external support.

Authors' Contributions Statement:
All authors contributed equally to the work and approved the final version of the manuscript.

Acknowledgment:
The authors gratefully acknowledged the reviewers and the Editor in-chief for their comments and necessary suggestions.

Appendix

$$A_{1n} = \frac{B_2 r_n^2 - R}{B_1}, A_{2n} = \left[\frac{B_4}{B_3\lambda}\left(1+\frac{1}{\beta}\right)r_n^2 + \frac{B_6 M^2}{B_3\lambda} + \frac{B_4}{B_3\lambda K}\right]$$

$$B_1 = \frac{(\rho C_p)_{thnf}}{(\rho C_p)_f}, B_2 = \frac{k_{thnf}}{k_f}, B_3 = \frac{(\rho)_{thnf}}{(\rho)_f}, B_4 = \frac{\mu_{thnf}}{\mu_f},$$

$$B_5 = \frac{(\rho\alpha_T)_{thnf}}{(\rho\alpha_T)_f}, B_6 = \frac{\sigma_{thnf}}{\sigma_f}$$

References

[1] W. Tan and T. Masuoka, "Stokes' First Problem for a Second Grade Fluid in a Porous Half-Space with Heated Boundary,"*International Journal of Non-Linear Mechanics*, vol. **40**, pp. **515-522, 2005**.

[2] C. Fetecau, D. Vieru, and C. Fetecau, "On Some Herical Flows of Oldroyd-B fluids," *Acta Mechanica*, vol. **189**, pp. **53-63, 2007**.

[3] D. Vieru, T. Hayat, C. Fetecau, and C. Fetecau, "On the first problem of Stokes for Berger's fluids. II: The case γ≥((λ²)/4) and

γ>((λ²)/4)," *Applied Mathematics and Compututation*, vol. **197**, pp. **76-86, 2008**.

[4] Z. Ziabakhsh and G. Domairry, "Analytical Solution of Natural Convection Flow of a Non-Newtonian Fluid Between Two Vertical Flat Plates Using Homotopy Analysis Method," *Communication in Nonlinear Science and Numerical Simulation*, vol. **14**, pp. **1868-1880, 2009.**

[5] T. Hayat, R. Naz, and M. Sajid, "On the Homotopy Solution for Poiseuille Flow of a Fourth Grade Fluid," *Communications in Nonlinear Science and Numerical Simulation*, vol**. 15**, pp. **581–589, 2010.**

[6] L. Rabecca, M. Siegel, K. D. Kimberly, M. Miller, and J. Ahmedin, "American cancer society," **2019**. [Online]. Available: https://scholar.google.com/citations?

[7] M. Jain, G. C. Sharma, and R. Singh, "Mathematical modelling of blood flow in a stenosed artery under MHD effect through porous medium," *International Journal of Engineering Transactions B: Applications*, vol. **23**, no. **3&4**, pp**. 243-251, 2010**.

[8] K. M. Sharma, K. Bansal, and S. Bansal, "Pulsatile unsteady flow of blood through porous medium in a stenotic artery under the influence of transverse magnetic field," *Korean-Australian Rheology Journal*, vol. **24**, no. **3**, pp. **181-189, 2012.**

[9] N. Shavastava, "Analysis of flow characteristics of the blood flowing through an inclined tapered porous artery with mild stenosis under the influence of an inclined magnetic field," *Journal of biophysics*, vol. **9**, p. **797142, 2014.**

[10] D. Kumar, B. Satyanarayana, K. Rajesh, D. Narendra, and K. Sanjeev, "Application of heat source and chemical reaction in magnetohydrodynamic blood flow through permeable bifurcated arteries with inclined magnetic field in tumor treatments," Journal of Result in Applied Physics, vol. **10**, no. **100151**, pp. **1-13, 2021**.

[11] E. E. Tzirtzilakis, "A mathematical model for blood flow in magnetic field," *Physics of Fluids*, vol. 17, no. 7, pp. 077-103, 2005.

[12] E. E. Tzirtzilakis, "Biomagnetic fluid flow in a channel with stenosis," *Physica D: Nonlinear Phenomena*, vol. **237**, no**. 1**, pp. **66-81, 2008.**

[13] M. A. Ikbal, S. Chakravarty, K. K. Wong, J. Mazumdar, and P. K. Mandal, "Unsteady response of non-Newtonian blood flow through a stenosis artery in magnetic field," Journal of Computational and Applied Mathematics, vol. **230**, no. **1**, pp. **243-259, 2009**.

[14] I. Pishkar, B. Ghasemi, A. Raisi, and S. M. Aminossadati, "Natural Convective Heat Transfer of Magnetite/Graphite Slurry Under a Magnetic Field," *Journal of Thermo-physics and Heat Transfer*, pp. **1-13, 2019.**

[15] T. Nazar and M. S. Shabbir, "Irreversibility analysis in the ternary nanofluid flow through an inclined artery via Caputo-Fabrizio fractional derivatives," *Results in Physics*, pp. **2211-3797(23)00785-4, 2023.**

[16] J. C. Chato, "Heat transfer to blood vessels," Journal of Biomechanical Engineering, vol. 102, no. 2, pp. 110–118, 1980.

[17] S. Shaw and P. V. S. N. Murthy, "Magnetic drug targeting in the permeable blood vessel: the effect of blood rheology," *Journal of Nanotechnology in Engineering and Medicine*, vol. **1**, no. **2**, pp. **021001–021011, 2010**.

[18] S. Maiti, S. Shaw, and G. C. Shit, "Caputo–Fabrizio fractional order model on MHD blood flow with heat and mass transfer through a porous vessel in the presence of thermal radiation," *Physica A: Statistical Mechanics and its Applications*, vol. **540**, p. **123149, 2020**.

[19] J. C. Misra and G. C. Shit, "Flow of a biomagnatic visco-elastic fluid in a channel with streching walls," *Journal of Applied Mechanics*, vol. **76**, no. **6**, p. **061006, 2009**.

[20] A. Mondal and G. C. Shit, "Transport of magneto-nanoparticles during electro-osmotic flow in a micro-tube in the presence of magnetic field for drug delivery application," *Journal of Magn. Magn*. Mater., vol. **442**, pp. **319–328, 2017**.

[21] S. Maiti, S. Shaw, and G. C. Shit, "Fractional order model for thermochemical flow of blood with Dufour and Soret effects under magnetic and vibration environment," *Colloids and Surfaces B: Biointerfaces*, vol**. 197**, p. **111395, 2021**.

